

LH power modulation experiment on JET

Y. Baranov, K. Kirov, M. Goniche, J. Mailloux, M.L. Mayoral et al.

Citation: [AIP Conf. Proc. 1187](#), 343 (2009); doi: [10.1063/1.3273763](https://doi.org/10.1063/1.3273763)

View online: <http://dx.doi.org/10.1063/1.3273763>

View Table of Contents: <http://proceedings.aip.org/dbt/dbt.jsp?KEY=APCPCS&Volume=1187&Issue=1>

Published by the [American Institute of Physics](#).

Related Articles

Comparisons between nonlinear kinetic modelings of simulated Raman scattering using envelope equations
[Phys. Plasmas 19](#), 013110 (2012)

Vlasov simulation in multiple spatial dimensions
[Phys. Plasmas 18](#), 122109 (2011)

Relativistic Bernstein waves in a degenerate plasma
[Phys. Plasmas 18](#), 092104 (2011)

A comparison of Vlasov with drift kinetic and gyrokinetic theories
[Phys. Plasmas 18](#), 064507 (2011)

Two-dimensional Vlasov simulation of electron plasma wave trapping, wavefront bowing, self-focusing, and sidelooss
[Phys. Plasmas 18](#), 052102 (2011)

Additional information on AIP Conf. Proc.

Journal Homepage: <http://proceedings.aip.org/>

Journal Information: http://proceedings.aip.org/about/about_the_proceedings

Top downloads: http://proceedings.aip.org/dbt/most_downloaded.jsp?KEY=APCPCS

Information for Authors: http://proceedings.aip.org/authors/information_for_authors

ADVERTISEMENT



The advertisement features the **AIP Advances** logo with a green and blue color scheme and orange spheres. It includes a "Submit Now" button and text about the journal's new open-access metrics and commenting features.

Explore AIP's new open-access journal

- Article-level metrics now available
- Join the conversation! Rate & comment on articles

Submit Now

LH power modulation experiment on JET

Y. Baranov^a, K. Kirov^a, M. Goniche^b, J. Mailloux^a, M.-L. Mayoral^a, J. Ongena^c, F. Nave^l and EDFA-JET contributors^{*}

JET-EDFA, Culham Science Centre, OX14 3DB, Abingdon, UK

^a*Euratom/UKAEA Fusion Association, Culham, UK*

^b*CEA, IRFM, F-13108 Saint-Paul-lez-Durance, France*

^c*Association EURATOM-Belgian State, LPP-ERM/KMS, Belgium*

Abstract. LH power modulation was recently used at JET to quantify experimentally the LH current drive efficiency and power deposition. A new approach was applied for the analysis of the amplitude and phase of electron temperature T_e perturbations $\delta T_e(k\omega_o)$ at different harmonics k of the modulation frequency ω_o . A solution of the Fokker-Planck equation combined with heat transport modelling was used to study the dependence of the ratio of the perturbation of different harmonics k and n , $\delta T_e(k\omega_o)/\delta T_e(n\omega_o)$, and the phase shift of the harmonics $\delta\phi(k\omega_o)$ on the plasma parameters and electron distribution function plateau width, which is directly connected to the current drive efficiency. The results of the modelling were compared with the experimental data to estimate the current drive efficiency. In addition, LH power deposition profiles were deduced from the radial dependence of $\delta\phi(\omega_o)$. The maximum of the LH power deposition becomes more peripheral and with a reduced current drive efficiency at higher densities. In H-Mode plasmas, at pedestal densities above the LH accessibility limit, a large fraction of the power is absorbed beyond the separatrix. Finally, the experimental power deposition profiles are more peripheral than the calculated ones obtained from combined ray tracing and Fokker-Planck modelling. The experimental results indicate that the LH power spectrum in the plasma is modified, with more power in the high $N_{||}$ components.

PACS: 52.35.Hr, 52.40.Db, 52.50.Sw

EXPERIMENTAL OBSERVATIONS

LH waves at 3.7GHz were launched in JET L- and H-Mode plasmas at line-averaged densities between 10^{19} m^{-3} and $3.5 \times 10^{19}\text{ m}^{-3}$ at $B_t = 2.2, 2.7, 3.4\text{T}$. Peak electron density varied in these experiments between 1 and $5 \times 10^{19}\text{ m}^{-3}$. The LH power was square modulated (modulation depth between 70 and 90%) at a modulation frequency $\omega_o/(2\pi) \approx 42\text{Hz}$. The launched spectrum of the LH waves has a maximum at $N_{||}=1.84$ for 0° antenna phasing. The electron temperature profile $T_e(r)$ was measured with the ECE diagnostic in the region of large optical depth $\tau >> 1$. Figure 1 shows the modulated LH power, the time variation of T_e at different radii, the phase shift between the electron temperature and modulated LH power $\delta\phi(\omega_o) = \phi(T_e(\omega_o)) - \phi(P_{lh}(\omega_o))$, the normalized amplitude of the first harmonic $A(\omega_o) = \delta T_e(\omega_o)/\delta P_{lh}(\omega_o)$, where $\delta P_{lh}(\omega_o)$ the amplitude of P_{lh} variation and $T_e(r)$ and $n_e(r)$ profiles. The effect of suprathermal emission was estimated [1] as relatively small for a moderate to high density plasmas above $1.5 \times 10^{19}\text{ m}^{-3}$. Its contribution becomes considerable in at the plasma periphery, where the optical depth $\tau < 1$, as

* See the Appendix of F. Romanelli et al., Fusion Energy Conference 2008 (Proc. 22nd Int. FEC Geneva, 2008) IAEA, (2008)

shown in Fig. 1e for $R>3.7\text{m}$. The calculation of $\delta\phi(\omega_o)$ and $A(\omega_o)$ is not valid in this region.

The maximum of the power deposition profile correlates with the maximum of the profile of $\delta\phi(\omega_o)$. Heat transport modelling with TRANSP and JETTO shows [2] that the LH power deposition profile is peaked in the vicinity of $\max(\delta\phi(\omega_o))$ with a small possible shift (a few cm) towards the plasma core. The maximum is broad with a half width of the order of half the minor radius. Figure 2 shows the location of $\max(\delta\phi(\omega_o))$ for a series of pulses at different magnetic fields and densities.

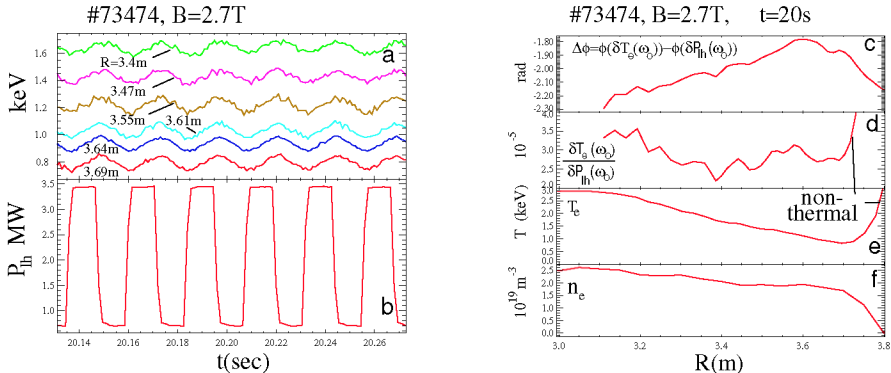


FIGURE 1. a) T_e perturbations at different radii caused by (b) modulated LH power. (c) The phase shift $\delta\phi(\omega_o) = \phi(T_e(\omega_o)) - \phi(P_{lh}(\omega_o))$ and (d) normalized amplitude $A(\omega_o) = \dots$ e) T_e and f) n_e profiles.

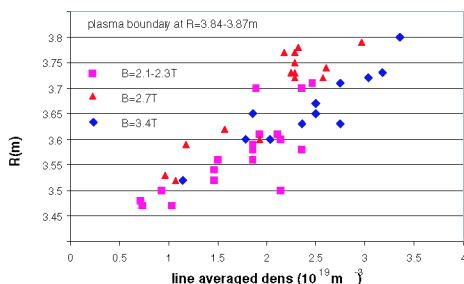


FIGURE 2. Position of $\max(\delta\phi(\omega_o))$ vs. line averaged density. Peak of the power deposition located near $\max(\delta\phi(\omega_o))$ moves to the plasma boundary with density increase. There is no significant difference between pulses at different B . T_e in the pulses varied in the region of $\max(\delta\phi(\omega_o))$ in the range of $0.6 < T_e < 2 \text{ keV}$, which may explain the vertical scattering of the points.

ANALYSIS OF THE DATA

A new approach has been proposed in this work to deduce the current drive efficiency by analysing the spectral characteristics of the phase $\delta\phi(k\omega_o)$ and the amplitude $\delta T_e(3\omega_0)$, $\delta T_e(\omega_o)$ of T_e perturbations when using modulated LH power. Transport analysis showed that in the case of pure heat transport the maximum phase delay of the first harmonic $\max(\delta\phi_{tr}(\omega_o))$ should vary between $-\pi/2$ for $\chi_e \rightarrow 0$ and $-\pi/4$ for $\chi_e \rightarrow 0$ [3]. For the χ_e values found in these experiments we find, again assuming pure heat transport that $\max(\delta\phi_{tr}(\omega_o))$ should change from -0.9 in case of low

density $\bar{n}_e \approx 10^{19} m^{-3}$ to -1.3 for high $\bar{n}_e \approx 3 \cdot 10^{19} m^{-3}$ [3]. The measured $\max(\delta\phi(\omega_o)) = -1.3$ at high density $\bar{n}_e \approx 3 \cdot 10^{19} m^{-3}$ [2]. In the example shown in Fig 1c we find however $\max((\delta\phi(\omega_o))) = -1.8$, which is outside the limiting values given above. The difference can be explained by the fact that the launched LH waves interact primarily with fast electrons. These electrons transfer power to the bulk electrons with some delay $\tau \propto (1/v_e)(V/V_{th})^3$ increasing with the velocity of the electrons V , where v_e is the collisional frequency of the thermal electrons.

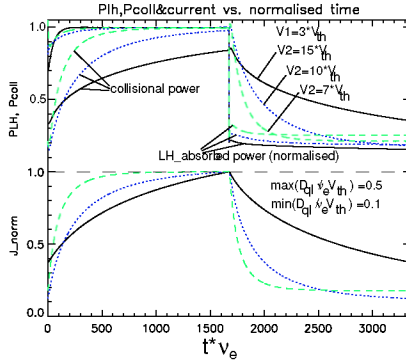


Figure 3. Absorbed LH and collisional power variation during one period of the modulation in pulse #77609, $T_e=0.8\text{keV}$, $n_e=2.2 \cdot 10^{19} m^{-3}$ at $R=3.63m=R(\max(\delta\phi(\omega_o)))$ and $\tau_n=2\pi v_e/\omega_o=3350$. Dependence on the $\max(D_{q1})$ is relatively weak. The normalized electric field in all cases was small $0.001 < E_n=eE/(v_e m V_{th}) < 0.003$ and did not affect visibly the results. The spectral characteristics of the collisional power depend mainly on the maximum ‘plateau’ velocity $V2$. Dependence on $V1$ is weak. It is typically close to 3.

Table 1. Results of 2D relativistic Fokker-Plank modelling for pulse #77609

$V2$	15	10	7	5
$\Delta\phi$	-0.86	-0.55	-0.28	-0.14
$\delta P_{col}(3\omega_o)/\delta P_{col}(\omega_o)$	0.18	0.22	0.28	0.32
$J/P(v_e \sqrt{m T_e} / e)$	81.5	35	21	15.2

Figure 3 shows time variation of the absorbed LH power, collisional power transferred from the fast tail electrons to the bulk and generated current as deduced from a solution of the 2D relativistic Fokker-Plank equation [4]. A dependence of the phase delay between the first harmonic of the collisional and applied power $\Delta\phi=\phi(P_{col}(\omega_o))-\phi(P_{lh}(\omega_o))$ and the ratio of the amplitudes of the third and the first harmonic of the collisional power $\delta P_{col}(3\omega_o)/\delta P_{col}(\omega_o)$ are shown in Table 1. The measured T_e perturbations are caused by $\delta P_{col}(k\omega_o)$, which in turn depends on the input LH power P_{lh} and the width of the plateau in the electron velocity distribution (localized between the lower value $V1$ and upper value $V2$ in units of V/V_{th}) as demonstrated in Figure 4 and Table 1.

Figure 4 shows the ratio $\delta P_{col}(3\omega_o)/\delta P_{col}(\omega_o)=G \delta T_e(3\omega_0)$, $\delta T_e(\omega_o)$ and $\Delta\phi$ deduced from the measurements at $R=R(\max(\delta\phi(\omega_o)))$ and from the modelling. Solid symbols correspond to $\Delta\phi=\phi(P_{col}(\omega_o))-\phi(P_{lh}(\omega_o))$ deduced from 2D relativistic Fokker-Planck modelling assuming that $V1=3$ and $V2=[c/(N_{acc} \cdot V_{th})]$, with N_{acc} defined by the local accessibility condition at the peak of the power deposition profile. The open symbols show $\delta\phi(\omega_o)=\phi(T_e(\omega_o))-\phi(P_{lh}(\omega_o))-\delta\phi_{tr}(\omega_o)$, where $\delta\phi_{tr}(\omega_o)$ and G are derived from TRANSP and JETTO modelling. The upper limit for $\delta\phi_{tr}(\omega_o)=-0.9$ and $G=3.1$ and the lower limits are -1.3 and 2.6, respectively. The triangles show the upper limit

for the experimental $\delta\phi(\omega_o)$ and $\delta P_{\text{col}}(3\omega_o)/\delta P_{\text{col}}(\omega_o)$ and the squares show the lower limit. The result of the modelling at low density is within the range of the measured $\delta P_{\text{col}}(3\omega_o)/\delta P_{\text{col}}(\omega_o)$ and $\delta\phi(\omega_o)$. At higher n_e the measured values are well above the modelled ones and the discrepancy increases with increasing density. Solid green circles represent results of the Fokker-Planck modelling for different values of V2 as shown in the graphs. At high density best agreement is reached at the lowest V2, which corresponds to the lowest current drive efficiency.

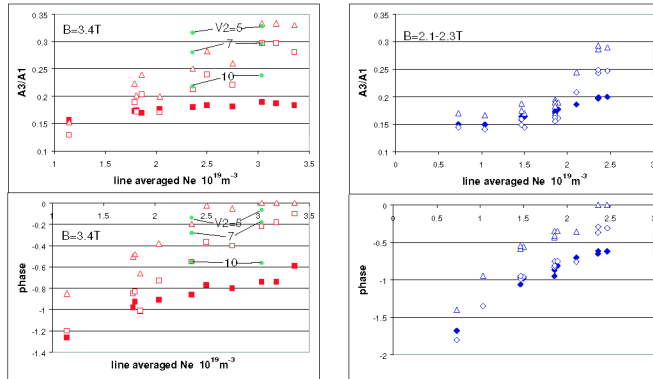


Figure 4. Measured (open symbols) and calculated (solid symbols) $A(3\omega_o)/A(\omega_o)$ and $\Delta\phi$ as functions of n_e . Open triangles are the upper and open squares and diamonds are lower limits of the measured functions.

Standard Ray-tracing [5] and Fokker-Planck modelling done for a number of experimental pulses shows that the modelled power deposition profile is shifted to the plasma core with respect to the measured power deposition profile.

Conclusions. LH Power deposition profiles were deduced by analyzing the spectral characteristic of T_e perturbations using LH power modulation. The peak of the profiles moves towards the periphery and current drive efficiency decreases when density increases as deduced from the transport and 2D relativistic Fokker-Planck modelling of the experiment. Power absorbed in the plasma becomes small when pedestal density reaches the accessibility limit. A standard ray-tracing and Fokker-Planck modelling predict more central profiles and higher current drive efficiency than found in the experiment.

ACKNOWLEDGEMENT

This work was funded partly by the United Kingdom Engineering and Physical Sciences Research Council and by the European Communities under the contract of Association between EURATOM and UKAEA. The views and opinions expressed herein do not necessarily reflect those of the European Commission. This work was carried out within the framework of the European Fusion Development Agreement.

REFERENCES

1. C. Sozzi et al, 'Studies on LH-generated fast electron tail using the oblique ECE diagnostic at JET'. this conf.
2. K.Kirov et al, "LH Wave Absorption and Current Drive Studies by Application of Modulated LHCD at JET". 36th EPS Conference on Plasma Physics, Sofia, Bulgaria. 2009
3. F.Leuterer et al, Nucl.Fusion 43, 744 (2003)
4. M.Shoucri, I.Shkarofsky, Comp.Phys.Comm. 82,287(1994)
5. Yu.F.Baranov et al Nucl.Fusion 36, 1036 (1996)